

Paper III

REPORT

Using the angle frequency method to detect signals of competition and predation in experimental time series

Gunnar Sandvik,^{1*} Christine M. Jessup,² Knut L. Seip¹ and Brendan J. M. Bohannan²
¹Department of Environmental Technology, Høgskolen i Telemark, Porsgrunn, Norway
²Department of Biological Sciences, Stanford University, Stanford, CA, USA
 *Correspondence: E-mail: gunnsa2@frisurf.no; gunnar.sandvik@dalen.vgs.no

Abstract

Identifying interactions among organisms is central to the study of ecology. The Angle Frequency Method (AFM) allows the detection of interactions in time series data. The AFM takes pairwise data plotted in phase diagrams and identifies signals (vector directions in phase diagrams) associated with particular interactions. Using microbial experimental systems consisting of predators (bacteriophage T4) and prey/competitors (strains of *Escherichia coli*), we demonstrate that the AFM can identify predator–prey and competitive interactions. The level of control afforded by such microbial experimental systems allows direct tests of the utility and robustness of the AFM. Signals of predation were distinct from signals of competition, with the strongest signal of predation corresponding to the collapse of the predator population at low prey densities. Signals of competition reflected the difference in competitive strength between the superior and the inferior competitors. In addition, the effects of invasion and resource enrichment on interactions in the laboratory communities were detectable using the AFM. Our analyses support results from model simulations and analyses of lake time series by identifying similar sets of signals characteristic of predation and competition, and demonstrate that the AFM is an effective tool in rigorous studies of time series.

Keywords

Predation, competition, time series, chemostat, phage, phase portrait.

Ecology Letters (2004) 7: 1–13

INTRODUCTION

Interactions among organisms form the cornerstone of community ecology, yet identifying and quantifying interactions in a particular community can be challenging. Multiple interactions, weak interactions, indirect interactions, and environmental forcing can mask pairwise interactions in many natural systems. To tease apart interactions in such complex systems, researchers have applied two approaches. First, manipulations such as removal experiments can identify key direct and indirect interactions (Paine 1974; Lubchenco 1978). However, such manipulations are not feasible in most natural systems, and even when feasible, their results can be difficult to interpret (Raffaelli & Moller 2000). The second approach involves the analysis of time series data from long-term monitoring programs by fitting mechanistic models (e.g. Kretzschmar *et al.* 1993), using statistical approaches, or both to identify patterns that are indicative of particular interactions (e.g. Stenseth *et al.* 1997;

Jost & Arditi 2000, 2001; Turchin *et al.* 2000; Berryman 2001; Berryman & Turchin 2001). However these approaches either require substantial information about the community of interest (e.g. to parameterize mechanistic models), or rely on simplifying assumptions (e.g. linear relationships between response and predictor variables) that are often violated in ecological time series. Recently, an approach – the Angle Frequency Method (AFM) – has been proposed that avoids these difficulties (Seip & Pleym 2000).

The AFM builds upon the rich tradition of graphical analysis of predation and competition in ecology (Lotka 1925; Volterra 1926; Rosenzweig & MacArthur 1963; MacArthur 1972). The AFM involves the analysis of time series data plotted as phase portraits (Gilpin 1973; Seip 1997; Seip & Pleym 2000), diagrams in which the densities of two populations are plotted as points in the positive x – y space (e.g. where x represents prey density and y the predator density), and a line is drawn connecting successive points. The rationale for this approach is that different types

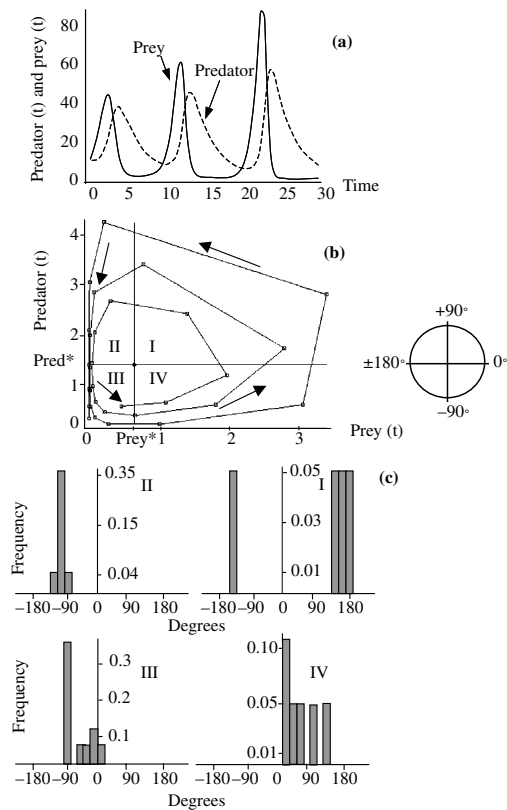


Figure 1 The successive steps in applying the AFM to a typical simulated predator–prey interaction. (a) Simulated predator–prey population cycles with prey represented by the solid line and predator by the dashed line. (b) The simulated time-series data converted into a predator–prey phase portrait, showing the vectorized trajectory. This phase portrait can be divided into four quadrants delineated by the steady-state average population densities ($Prey^*$ and $Pred^*$), calculated here as the average abundance of populations. In quadrant 1 (upper right), the abundance of both species is above their average abundance and in quadrant 3 (lower left), both species are below their average abundance. Quadrants 2 and 4, represent regions of the time series where one species is above and the other below its average abundance. In each of these quadrants, the direction of vectors between successive time points (measured with reference to the positive x -axis) is determined. In this example, predator–prey interactions are predicted to generate positive angles of 120 – 140° in the first quadrant and negative angles of $c. -70$ to -90° in the second quadrant. The arrows indicate the approximate average angle for each of the four quadrants (see protractor to estimate angle). (c) The vector directions are sorted into angle classes (sectors of 18°) and summarized in histograms, which serve as ‘fingerprints’ for interactions. For predator–prey interactions using simulated data, the angle histograms reveal primarily positive angle classes in the first and fourth quadrants and negative angle classes in the second and third quadrants of the phase portrait, due to the counter-clockwise direction of a prey–predator trajectory (Sandvik *et al.* 2002).

of ecological interactions will show unique patterns in phase portraits. Thus, from time series data, signals associated with a particular interaction can be identified.

Consider the interaction between predators and prey. Figure 1 shows the successive steps in applying the AFM to a typical simulated predator–prey interaction. Because predator–prey population cycles are often out of phase (prey increase before predators; Fig. 1a), phase portraits of predator–prey time series exhibit counter-clockwise rotation when the prey is depicted on the x -axis and the predator on the y -axis (Gilpin 1973; Seip & Pleym 2000; Fig. 1b). This phase portrait can be divided into four quadrants that meet at the average abundance of each population. In each of these quadrants, the direction of vectors between successive time points is measured relative to the positive x -axis (see Fig. 1 legend for details). These vector directions are then sorted into angle classes and summarized in histograms, which serve as ‘fingerprints’ for interactions (Fig. 1c). By applying multivariate statistics, we are able to determine the degree of clustering or separation between phase portraits

and we can identify signals associated with particular interactions.

The AFM takes relatively qualitative patterns (e.g. rotation of a trajectory), and distills this information into quantitative signatures of a predator–prey interaction. For example, consistent counter-clockwise rotation in a phase portrait is indicative of a predator–prey interaction, and this trend is reflected in the distribution of angles in the angle histograms generated for each quadrant. In the case of two populations competing for a shared resource in a constant environment, we expect the superior competitor to ultimately exclude the inferior competitor. Seasonality can impose rotation in a phase portrait of two competitors; however, unlike phase portraits of predation, there is no predominant direction to this rotation. Based on these fundamental differences in interactions, as well as more subtle differences in the shape of the phase portrait trajectories, the AFM is capable of differentiating predation and competition. The method is also capable of identifying a lack of interaction in paired time series data. A pair of non-interacting species would yield a time series in which points are randomly distributed, which would, in turn, yield a uniform distribution of angles and a lack of clustering in the subsequent statistical analyses.

The AFM successfully differentiated predation, competition, mutualism and facilitation in simulated time series that were based on simple Lotka Volterra-type models in a seasonal environment (Sandvik *et al.* 2002). However, the ability of the AFM to distinguish interactions in biological systems requires further testing. The first attempt to apply the AFM to real data involved analysing observational lake plankton data (from several lakes) to determine whether predation and competition could be differentiated. The results suggested the existence of unique predation and competition signals in these time-series, but these signals were difficult to interpret (Sandvik *et al.* 2003). Signals in lake time series data identified by the AFM could be due to biotic interactions (e.g. an increase in zooplankton causing a decrease in phytoplankton) or dynamic abiotic forces (e.g. lower temperatures later in the season), and resolving these different forces is challenging. We sought to test the AFM in a system without these potentially confounding abiotic factors and look for robust signatures of biotic interactions in real time series data.

Microbial experimental systems offer the ability to conduct controlled, replicated experiments over relatively long time periods and at large relative spatial scales (Jessup *et al.* 2004). Microcosms can be inoculated with defined communities and defined resources. Communities of organisms with known characteristics (e.g. strong competitors, weak competitors, and predators) can be assembled, and populations are readily sampled and enumerated. Microorganisms can have short generation times and attain large populations in the laboratory, allowing direct explorations of long-term (multi-generational) ecological interactions. Here, we apply the AFM to laboratory communities to determine if there are general signals that consistently distinguish interactions, and to determine whether the AFM is sufficiently sensitive to detect changes in these interactions. In addition, the level of control in these experimental systems, combined with modelling, permits exploration of the robustness of the method. For example, we added different levels of error to actual time series data to determine whether signals of interaction can be differentiated in the presence of sampling error and environmental variability. If the method works in these more controlled experimental systems, our conviction that the AFM is a valuable tool for detecting ecological interactions and shifts in interactions in field data is strengthened.

We used microbial communities consisting of bacteriophage and bacteria to generate time series data for pairs of species in these communities. We assembled three-population communities containing two competitors and a predator that attacks one of the competitors. There are several reasons for this design. First, it allows us to work with relatively complex communities, where pairwise interactions are imbedded amidst other interactions. The second

reason for this choice of communities is practical. Long-term coexistence between competitors is facilitated by a predator feeding on the superior competitor. Finally, these types of systems have been previously studied and there are clear predictions for the effects of perturbations on community structure and dynamics. For example, increasing resource levels in a community consisting of only sensitive bacteria and phage, yields a large increase in the phage population, a slight increase in the sensitive bacterial population and a destabilization of both populations (Bohannan & Lenski 1997, 1999; Bohannan *et al.* 2002). In contrast, the effect of enrichment on a community containing phage-resistant bacteria, phage-sensitive bacteria and phage, yields an increase in the resistant population, no change in the abundance of phage or sensitive bacteria, destabilization of phage and sensitive bacteria, and stabilization of the resistant population (Bohannan & Lenski 1999). Mathematical models show that the magnitude of the cost of predator-resistance has important implications for the response of these communities to enrichment (Bohannan *et al.* 2002).

We evaluated the utility of the AFM in four ways. First, we explored whether the AFM can distinguish predation from competition in time series and whether we can identify the main signals (characteristic angles) from these analyses and evaluate their strength. Second, we explored the limits of the AFM. This was accomplished by determining whether the AFM can distinguish signals of competition and predation over long time scales in complex communities with transient dynamics, and whether the AFM can detect interactions in time series amidst artificially imposed error. Third we used the AFM to study ecological issues that are important in community ecology and ecosystem management. We studied the effects of resource enrichment on the signal strength and quality by comparing communities that differ in resource input. We also explored whether differences in relative competitive ability result in signals of different strength in a mixed community. Finally, we investigated the ability of the AFM to detect invasion from experimental time series. Throughout these analyses, we demonstrate not only that the AFM is a robust method for distinguishing interactions in mixed communities, but also that it is capable of detecting subtle shifts in interactions.

MATERIALS AND METHODS

Organisms

Our experiments used the virulent bacteriophage T4 as a model predator and three strains of *Escherichia coli* that differ in their competitive ability and bacteriophage vulnerability. We designated the *E. coli* strains as 'competitor-1', which is

susceptible to T4 (REL607; Lenski *et al.* 1991), 'competitor-2', which is invulnerable to attack by T4 (REL6584; Bohannan & Lenski 1999) and 'competitor-3' (derived from REL606; Lenski *et al.* 1991), which is also invulnerable to T4. Resistance to bacteriophage often confers a competitive cost in the absence of bacteriophage (Lenski & Levin 1985; Lenski 1988). The competitive disadvantage for the invulnerable strains used in this project was determined through competition with the phage-sensitive ancestor in phage-free glucose-limited chemostat environments (Bohannan & Lenski 1997). Based on these competition experiments, the three competitors used in this study can be ranked in order of decreasing competitive fitness with competitor-1 (T4-sensitive) as most fit, competitor-2 (T4-resistant) exhibiting intermediate competitive fitness, and competitor-3 (T4-resistant) as least fit. Additionally, competitor-1 harbours a competitively neutral genetic marker conferring the ability to utilize the sugar arabinose (Lenski *et al.* 1991; Bohannan & Lenski 1999). The ability to utilize arabinose allowed the T4-sensitive competitor (competitor-1) to be distinguished from the two T4-resistant competitors (competitor-2 and competitor-3).

Laboratory model system

Communities of bacteriophage and bacteria were maintained under continuous culture conditions in glucose-limited chemostats, as described by Bohannan & Lenski (1997). Briefly, chemostats were supplied with Davis minimal broth supplemented with glucose and $2 \mu\text{g L}^{-1}$ thiamine hydrochloride. Chemostat volumes were maintained at 30 mL and the dilution rate at 0.2 turnovers per hour. Temperature of the chemostats was maintained at 37 °C.

All chemostat communities contained populations of bacteriophage T4 and the T4-sensitive superior competitor (competitor-1) in addition to a T4-resistant population (either competitor-2 or competitor-3) (Fig. 2a). The T4-sensitive and T4-resistant bacterial populations competed for the limiting resource (glucose) while bacteriophage T4 attacked the superior competitor (competitor-1). Chemostats contained one of three possible community configurations, which we labelled 2_{H} , 2_{L} , and 3_{H} . The numeric term refers to whether the T4-resistant competitor in the community is competitor-2 or competitor-3, and the 'H' and 'L' indicate the input concentration of limiting resource, where 'H' represents high input concentration 0.5 mg L^{-1} and 'L' represents a low glucose concentration of 0.1 mg L^{-1} . For example, configuration 2_{H} communities contain competitor-2, competitor-1 and bacteriophage T4 with a high input concentration of the limiting resource. Chemostat runs consisted of blocks of six to eight chemostats run simultaneously. Chemostats in a run were

inoculated at the same time and replicate communities received resources from the same reservoir of media. Community configurations were replicated two- or threefold within a chemostat run. We analysed three chemostat runs described as 'short-term', which were run for 159–191 h (*c.* 32–38 predator generations), and one 'long-term' run that was maintained for 631 h (*c.* 126 predator generations).

Population densities of bacteria and bacteriophage were determined twice daily by diluting samples and plating on selective media (as described in Bohannan & Lenski 1999). In brief, competitor-1 was enumerated by dilution and plating on Davis minimal agar supplemented with $2 \mu\text{g L}^{-1}$ thiamine hydrochloride and $4 \times 10^3 \text{ mg L}^{-1}$ arabinose. This media allows the growth of competitor-1, which can utilize arabinose but prevents the growth of competitors-2 and -3, which are unable to utilize arabinose. Samples were mixed with heat-killed REL607 cells to inactivate free bacteriophage (Carlson & Miller 1994; Bohannan & Lenski 1999). Competitors-2 and -3 were plated on Davis minimal agar supplemented with $2 \mu\text{g L}^{-1}$ thiamine hydrochloride and $4 \times 10^3 \text{ mg L}^{-1}$ glucose in the presence of concentrated bacteriophage T4 lysate, which killed T4-sensitive cells (*i.e.* competitor-1; Bohannan & Lenski 1999). To plate T4, samples were first treated with chloroform to kill bacterial cells and then plated on a lawn of T4-sensitive bacteria, where individual viral particles formed countable clearings in the lawn or 'plaques' (Carlson & Miller 1994).

Analytical methods

To analyse the time series data, we used the Angle Frequency Method (AFM) originally developed by Seip (1997), and described in full by Seip & Pley (2000) and Sandvik *et al.* (2002). Briefly, we generated phase portraits from the time series data for pairs of species in a given interaction. In each of the four quadrants delineated by average population density, we identified the angle formed by the trajectory between two time points and the *x*-axis (Fig. 1b). These angles were sorted into angle classes (sectors) of 18° , yielding frequency distributions with 21 bars (one bar representing one signal and the height of the bar suggestive of signal strength, details below) per quadrant (Fig. 1c). The resulting histograms (four generated per pair of time series) were then compared to identify relevant signals (vector directions in phase portraits, associated with particular interactions). We used principal component analysis (PCA) to analyse these angle histograms (Unscrambler, version 6.11 b, Waterloo, Canada, CAMO ASA; Maple V, Release 5, Waterloo Maple, Inc.).

From the PCA scores generated by the AFM we calculated centre-centre distance (D) and score range (R_s) for any two groups of data to be compared. D was calculated as

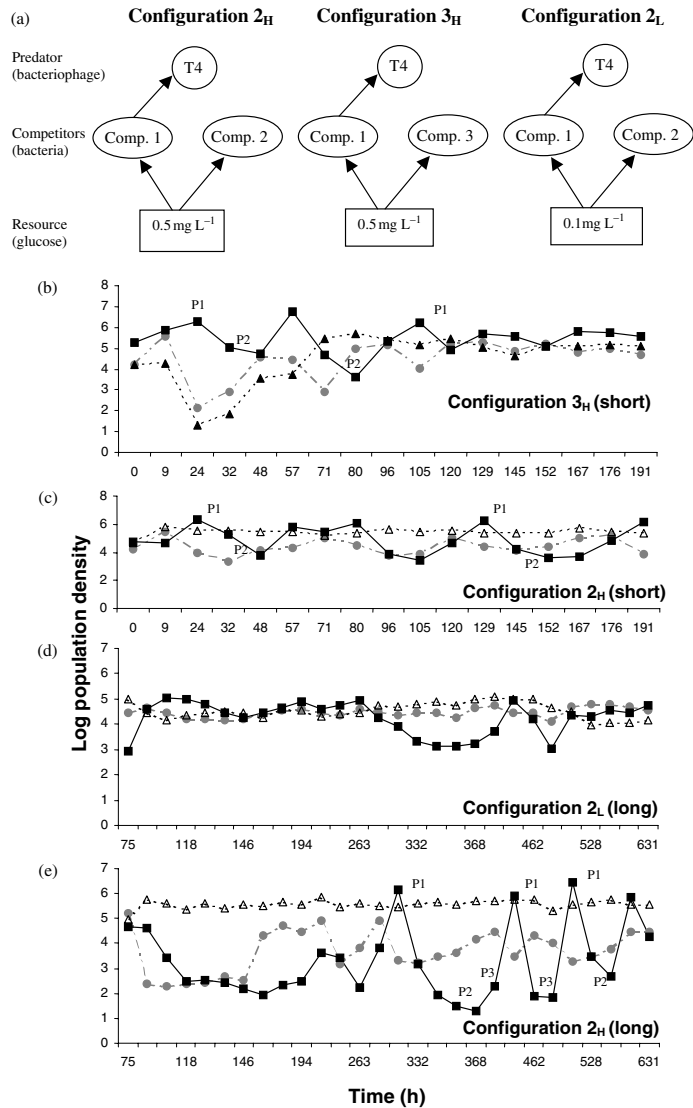


Figure 2 Experimental design and representative time series data. (a) Design of the three microbial system configurations analysed. A solid line between *E. coli* strains and phage T4 indicates that the strain is sensitive to the phage. The lack of connection between a bacterial strain and phage indicates that the strain is fully resistant to phage attack. (b–e) Log (base 10) population densities (*y*-axis) over time (*x*-axis) representing typical chemostats from short-term chemostat runs (b and c), and long-term runs (d and e). Solid squares represent the predator, bacteriophage T4; grey circles represent T4-vulnerable competitor-1; solid triangles represent T4-resistant competitor-3 (lowest competitive fitness); open triangles represent T4-resistant competitor-2 (intermediate competitive fitness). Individual points represent one sampling. Labeled regions of the time series (e.g., P1, P2) correspond to regions where interaction signals were identified and are discussed in the text.

$$D = |g_1| + |g_2|, \quad (1)$$

where g_1 is the average score of group 1 and g_2 is the average score for group 2 along a given PC-axis. R_n was calculated as

$$R_n = |S_{\min}| + |S_{\max}|, \quad (2)$$

where S_{\min} is the lowest score and S_{\max} is the highest score (irrespective of groupings among scores) along a given PC-axis. Discrimination ($D\%$) was then calculated as

$$D\% = \frac{D \times 100}{R_n}. \quad (3)$$

A $D\%$ value of 100 indicates that scores are separated as two distinct groups at opposite sides along the PC axis. A $D\%$ value of 0 represents a random distribution of scores. $D\%$ values in the range 10–15 were found to be visually detectable by inspection of score plots.

PCA loadings relate the variables (here the 84 angle classes) to the scores. Based on loadings associated with g_1 and g_2 scores evaluated for each of eight systems analysed, we defined signal strength (S_s):

$$S_s = R_s * E_s, \quad (4)$$

where R_s is representability and E_s is exclusivity of a signal over the systems analysed. R_s was calculated as

$$R_s = \frac{n_s}{N}, \quad (5)$$

where n_s is the number of systems in which a certain signal was characteristic. N is the number of systems analysed. Thus, higher R_s values (range 0–1) indicate that a signal occurs frequently. E_s was calculated as

$$E_s^{\text{comp}} = \frac{n_s^{\text{comp}}}{n_s^{\text{comp}} + 1}, \quad E_s^{\text{pred}} = \frac{n_s^{\text{pred}}}{n_s^{\text{pred}} + 1}, \quad (6)$$

where n_s^{comp} is the number of systems in which a certain signal was characteristic for competition and n_s^{pred} is the corresponding number for predation. E_s (range 0–1) gives high weight to signals that are characteristic for one interaction but not the other.

Signal strength (S_s) measures the degree to which a particular signal is representative of an interaction (predation or competition, in this study) and exclusive to one interaction and not the other. High S_s values (range 0–8 here) point to signals that are good candidates for identifying a given interaction type. To compare dynamics before and after a potential shift we use cumulative S_s values (ΣS_s):

$$\Sigma S_s = \sum_i^j S_{s_i}, \quad (7)$$

where i is the S_s value of the i th signal associated with the j th interaction (predation or competition). ΣS_s values measure cumulative strength of signals in particular ‘sub-analyses’ (e.g. segments of time series) relative to the S_s values identified from several analyses of full length time series. For example, high ΣS_s before a shift in dynamics and low ΣS_s after a shift in dynamics suggest that signals of interactions decay (or become less typical).

Robustness of the AFM

To address whether the AFM method can distinguish predator–prey from competitive interactions we applied the AFM to eight sets of time series generated from our experimental communities. Six sets came from the short-term chemostat runs (2_H and 3_H communities in each of three blocks) and two sets from the long-term chemostat runs (2_H and 2_L communities).

To determine whether the length of time series affected discrimination between predator–prey and competitive

interactions, we compared time series data generated from short-term and long-term chemostat runs. To explore the effect of time series length on the detection of interaction signals we applied the AFM to segments of data from the long-term configuration 2_H time series, using data from $t = 313$ to $t = 631$, which reflects ≈ 3.5 predator–prey cycles, where the dynamics are fairly stable.

To explore the effect of time series length on our analyses of enrichment, we generated angle frequencies for both full-length time series and time-series segments at low and high resource levels and averaged these across time-series length and nutrient level. Signals from high- and low-productivity communities were averaged across replicate chemostats for both segments of time series and the full-length time series.

Because time series from microbial experimental systems are relatively clean compared with those generated by observational field data, we added different levels of random error to experimental data to test whether the AFM could differentiate interactions in the presence of sampling error and environmental variability. We focused on the high nutrient, full-length time series (2_H), which yielded the best discrimination values of all our analyses ($D\%$ PC1 = 88) and offers a baseline for studying how increased levels of error influence results of the AFM. Both constant and proportional error was imposed on the full-length time series from the 2_H communities. Constant error, independent of population densities, was imposed on the time series by selecting from a normal probability function with a mean of zero and different levels of standard deviation (SD), expressed in the original data units [colony forming units (cfu)] and as a percent of the grand average density of each of the three populations across replicate runs. Proportional uniform error (dependent on the magnitude of each time point) was imposed with a random number generator using the whole numbers over the range (–5 to +5); if the random number was 0 the time point was unchanged, if it was –5 the time point was maximally reduced and if it was five the time point was maximally increased. First, the random number was multiplied by a relevant fraction of a given time point (e.g. 3%), producing a positive or negative ‘error’ of up to 15% (3 multiplied by 5) of the original value. In the second step, this ‘error’ was added to the original value. The AFM was applied to the resultant time series to determine discrimination between predation and competition.

Detecting shifts in interactions

To determine the effect of nutrient enrichment on signal strength and quality, we compared community configurations differing in resource input concentration. We analysed three replicate 2_L communities and two replicate 2_H communities to explore the effects of enrichment. (We only analyse two replicate 2_H communities, because in the third

replicate, the density of bacteriophage repeatedly cycled below the detection limit, thereby preventing the generation of angle-frequency histograms for this community.)

To determine whether differences in bacterial competitive ability can be detected in time series by AFM, we compared competition phase portraits from low-competitor-fitness (configuration 2_H) communities with those from high-competitor-fitness (configuration 3_H) communities (Fig. 2a).

To determine whether AFM is able to detect invasion, we analysed several chemostat runs in which we observed a dramatic shift in population dynamics that was likely due to invasion by an evolved bacterial strain. The shift was consistent with the expected dynamics following invasion by a derivative of competitor-3 exhibiting higher competitive fitness (Bohannan & Lenski 1999; Bohannan *et al.* 2002). We applied the AFM to sections of these time series, before and after $t = 80$ h, at which time a visible change in the dynamics occurred in the configuration 3_H communities (Fig. 2b).

RESULTS

Population dynamics

All chemostat configurations exhibited visually recognizable patterns of prey–predator dynamics (i.e. prey and predator densities oscillated with the same period, but with a slight lag between the predator and prey trajectories) (Fig. 2b–e). Similarly, for competition, one competitor’s trajectory had a tendency to be the mirror image of the other competitor’s trajectory (see Fig. 2c). The competitive fitness of predator-resistant bacterial strains appeared to significantly affect population dynamics. Competitor-2 has a higher competitive fitness than competitor-3 and this difference translated into distinct community dynamics in configurations 2_H and 3_H respectively. In configuration 2_H communities, populations exhibited stable oscillations (Fig. 2c); 3_H communities exhibited oscillations of decreasing amplitude and converged to the stable coexistence of all strains (Fig. 2b). The effects of resource enrichment on population dynamics were visible in long-term chemostat runs from configurations 2_H and 2_L (e.g. compare Fig. 2d,e). Oscillations of predator and prey populations were much more pronounced and the average population density of phage-resistant bacteria was tenfold higher in the enriched communities.

Identification of predation and competition signals

Scores for predation and competition formed distinct clusters in PCA plots. For the short-term chemostat runs, we found that $D\%$ PC1 values were high, indicating good discrimination between predation and competition scores (range 52–70, Table 1).

Table 1 Summary of discrimination between predation and competition. PCA scores from short-term and long-term chemostat runs

	Duration of chemostat run			
	Short-term run		Long-term run	
Glucose level (mg L ⁻¹):	0.5	0.5	0.1	0.5
Community configuration	3 _H	2 _H	2 _L	2 _H
Replicate communities (<i>n</i>)	8	8	3	3
<i>Discrimination between predation and competition scores</i>				
Segment of time series				
$D\%$ PC1	55–70	52–62	17	77
$D\%$ PC2	21–42	21–52	10	5
Full-length time series				
$D\%$ PC1	55–60	47–73	61	88
$D\%$ PC2	4–45	2–57	18	10

$D\%$ PC1 and $D\%$ PC2 indicate level of clustering in PCA scores along principal component 1 (PC1) and principal component 2 (PC2), respectively. Higher $D\%$ values reflect better separation of PCA scores. A $D\%$ value of 100 indicates that scores are separated as two distinct groups at opposite sides along the PC axis. A $D\%$ value of 0 represents a random distribution of scores. For short-term chemostat runs, data are summarized as ranges of discrimination values from three blocks of chemostat runs, with each community replicated two- or threefold in each block. For the long-term runs, discrimination values are presented as single values reflecting discrimination between competition and predation scores for communities replicated threefold within the experiment.

For the long-term chemostat runs, communities in chemostats with low glucose input concentration (configuration 2_L) scores clustered poorly along PC1 ($D\%$ PC1 = 17). In contrast, scores from communities at high glucose input concentration (configuration 2_H) clustered well along PC1 ($D\%$ PC1 = 77).

Several signals distinguished predation from competition. The strongest distinguishing signal was P1 (Fig. 3a, quadrant II), which reflects the early stage of the predator collapse, when the predator decreases rapidly from high numbers while the prey also declines. Signal P2 reflects the late stage of the predator collapse, when both populations are low and the rate of predator decline is low while the rate of prey growth is high. Signal P3 reflects the early predator build-up stage (i.e. the predator grows very fast when prey numbers are high). In general, the predator–prey signals confirmed the counter-clockwise rotation in phase portraits for a predator and its prey.

The strongest signals of competition were C1 and C2 (Table 2 and Fig. 3b). Signal C1 reflects the situation when both competitors are rare and the superior competitor

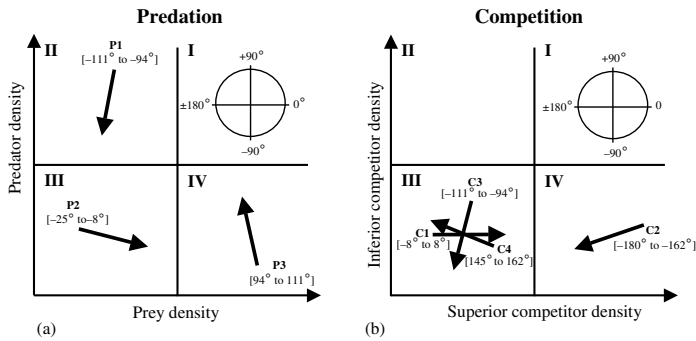


Figure 3 Predation and competition signals identified by the AFM. (a) Predation signals identified by applying the AFM to short-term time series data. (b) Competition signals revealed by similar analysis. The arrows show the approximate angle of the most characteristic angle brackets identified for each interaction (see text and Fig. 1). I, II, III and IV designate quadrant numbers. Coordinates for angle measures provided in quadrant I.

Predation				Competition			
Quadrant [range of angles]	Signal ID	Number of time series	\mathcal{S}_s	Quadrant [range of angles]	Signal ID	Number of time series	\mathcal{S}_s
II [-111 to -94]	P1	6	4.5	III [-8 to 8]	C1	4	2.0
III [-25 to -8]	P2	5	1.6	IV [-180 to -162]	C2	4	2.0
IV [94 to 111]	P3	3	1.1	III [-111 to -94]	C3	3	1.1
II [-94 to -77]		3	0.6	III [145 to 162]	C4	3	1.1
III [-94 to -77]		3	0.6	III [-180 to -162]		2	0.5
III [-77 to -60]		2	0.5	III [43 to 60]		2	0.5

Number of time series reflects the number of time series in which a given angle bracket was identified out of the eight systems. Signals with \mathcal{S}_s values > 1 are given signal IDs and are discussed in the text.

increases rapidly while the inferior competitor remains relatively constant. Signal C2 originates from the situation where the superior competitor decreases rapidly from high population density while the inferior competitor also decreases, but from low density. Signal C3 reflects the situation where both competitors decrease at low population densities, but the inferior competitor decreases much faster than the superior. Signal C4 reflects slow growth of the inferior competitor paired with rapid decline of the superior competitor at low densities of both populations.

Effects of enrichment on signal strength

Community configurations 2_H and 2_L differed only in the input of the limiting resource, with the input concentration for 2_H communities fivefold higher than that for 2_L communities. Discrimination was more than four times higher in the enriched communities ($D\%$ PC1 = 77) than in the low productivity communities ($D\%$ PC1 = 17) (Table 1). This reflects differences in dynamics that were readily observed in the time series (Fig. 2d,e). PCA loadings showed that the best identifiers of interactions in the enriched communities were signals P2 for predation and C3

for competition. For the low productivity communities, no signals could be identified from the time-series data because of the lack of clustering in PCA scores, as mentioned above.

Effect of differences in bacterial competitive fitness on system dynamics and signals

Competition and predation showed distinct signals in phase portraits from both low-competitor-fitness (configuration 2_H) and high-competitor-fitness (configuration 3_H) communities; discrimination between competition and predation signals was relatively high and quite similar in both configurations ($D\%$ PC1 = 69 and 67 in configuration 2_H and configuration 3_H chemostats, respectively; Table 3).

Comparing competition phase portraits from low-competitor-fitness (configuration 2_H) communities with those from high-competitor-fitness (configuration 3_H) communities revealed that competition between competitors-1 and-3 could be distinguished from competition between competitors-1 and-2 ($D\%$ PC1 = 75) (Table 3). This result is consistent with the observation that competition time series differed between these two configurations with 3_H communities exhibiting pronounced oscillations. The presence

Table 3 Effects of competitor fitness on predator–prey and competitive dynamics. Summary of discrimination values ($D\%$ PC1 and $D\%$ PC2) for competition and predation signals within and between community configurations and cumulative signal strength (ΣS_s) for segments of time series and full-length time series

	Interaction discrimination				Cumulative signal strength (ΣS_s)			
	Within community configurations		Between community configurations		Configuration 2 _H		Configuration 3 _H	
	$C_{2H} \times P_{2H}$	$C_{3H} \times P_{3H}$	$C_{2H} \times C_{3H}$	$P_{2H} \times P_{3H}$	<i>C</i>	<i>P</i>	<i>C</i>	<i>P</i>
Segment of time series								
$D\%$ PC1	67	69	75	9	0.29	9.30	7.00	8.83
$D\%$ PC2	11	13	21	55				
Full-length time series								
$D\%$ PC1	65	55	68	29	0.92	9.47	4.18	3.92
$D\%$ PC2	19	26	1	34				

C represents competition and *P* represents predation. For example, $C_{2H} \times P_{2H}$ compares discrimination between competition and predation in configuration 2_H communities. Higher $D\%$ values reflect better separation of PCA scores.

and strength of competition signals also differed between the two configurations. ΣS_s values were higher for configuration 3_H communities (signals C1 and C2), than for configuration 2_H communities (Table 3), however a shift in dynamics (discussed below) may have contributed to the weaker signal strength in 3_H communities.

A similar analysis of the predator–prey interactions in communities 2_H and 3_H revealed only subtle differences ($D\%$ PC1 = 9). Predation was characterized by a few strong signals in both configurations (P1 and P2; Table 3). The strength of predator–prey signals was similar in 2_H and 3_H communities when segments of time series were analysed; analysis of full-length time series revealed higher signal strength in 2_H communities (Table 3).

Detection of changes in dynamics following invasion

In all of the configuration 3_H chemostats containing lower-fitness competitor-3, we observed a shift in the dynamics of predator, prey and competitor approximately halfway through the experiment (Fig. 2b). Discrimination between configuration 3_H competition phase portraits generated before and after $t = 80$ was high ($D\%$ PC1 = 71); a similar comparison of predation phase portraits also revealed high discrimination ($D\%$ PC1 = 55). Configuration 2_H communities exhibited lower discrimination between phase portraits before and after $t = 80$ ($D\%$ PC1 = 42 for competition and $D\%$ PC1 = 33 for predation).

Evidence for a change in the configuration 3_H communities was further supported by a shift in signals and signal strength. Signals identified before $t = 80$ were consistent with typical signals identified above (P1, P2, C1 and C2) and exhibited high cumulative S_s values ($\Sigma S_s = 5.6$ for competition and $\Sigma S_s = 6.7$ for predation). However, after $t = 80$,

signals of competition could not be identified and signals of predation were atypical and weak ($\Sigma S_s = 0.6$). In contrast, when configuration 2_H communities were analysed similarly, signals were the same (P1, P2 and C1) and of similar strength before and after $t = 80$ ($\Sigma S_s = 6.1$ for predation and $\Sigma S_s = 2.0$ for competition, before and after $t = 80$).

Robustness of the AFM

We found that increasing the length of the time series analysed increased discrimination. Analyses that included 0.5, 1, 1.75 and 3.5 predator–prey cycles yielded discrimination values of $D\%$ PC1 = 29, 25, 38 and 83, respectively. Discrimination between predation and competition was higher at the higher resource level for segments of the time series and for full-length time series (i.e. separation between corresponding competition and predation scores was larger at higher resource levels; Fig. 4). Discrimination was also higher for full-length time series than for segments of time series. In summary, nutrient level had the largest effect on discrimination between competition and predation, but the length of the time series analysed was also important.

The effects of competitor fitness on community dynamics were largely unaffected by length of time series analysed. The discrimination between competition scores from the two configurations was similar in time series segments ($D\%$ PC1 = 75) and in full-length time series ($D\%$ PC1 = 68) (Table 3). Discrimination between predation scores from the two community configurations was slightly higher for full-length time series ($D\%$ PC1 = 29) than for segments of time series ($D\%$ PC1 = 9). Within-configuration discrimination between predation and competition was similar for time-series segments ($D\%$ PC1 = 67) and full-length time series ($D\%$ PC1 = 65) for configuration 2_H, and the

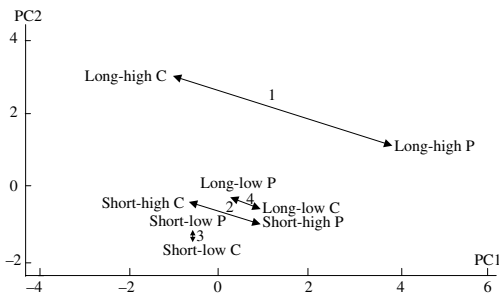


Figure 4 PCA score plot for the enrichment analysis (configurations 2_H and 2_L). The x -axis is PC1, the principal component that explains the highest portion of variation in the data (53% in this analysis); the y -axis is the second most important PC dimension (20%). Labels indicate the length of time series (short-term or long-term), nutrient level (high or low) and ecological interaction [predation (P), competition (C)]. Arrows reflect corresponding signals (i.e. predation–competition pairs). Arrow 1 is the long-term time series from high productivity chemostats, arrow 2 is the short-term time series from high production chemostats, arrow 3 is short-term time series from low production chemostats and arrow 4 is long-term time series from low productivity chemostats.

results were similar for discrimination between competition and predation in configuration 3_H communities ($D\%$ PC1 = 69 for segments and $D\%$ PC1 = 55 for full-length time series) (Table 3).

Analysis of time series modified to simulate sampling error and environmental variability suggests that the AFM is fairly robust. The results of imposing the same level of constant error to each time point in nine time series showed that predation could be distinguished from competition at error levels up to *c.* 50% (Table 4) and signals were unchanged as long as $D\%$ PC1 values are above 10–20. Analyses of time series with proportional error showed high discrimination between predation and competition at all

error levels analysed. It did not seem possible to distort the underlying pattern by using proportional error.

DISCUSSION

In our analyses, we have shown that the AFM systematically distinguishes predation from competition in experimental time series data from assembled microbial communities containing multiple interactions. Our results also demonstrate that events that are predicted by theory, such as the effects of invasion, enrichment and competitor fitness on population dynamics, can be detected by the AFM. We have identified typical signals for predation and competition based on the frequency at which signals for a particular interaction occur. We were able to identify several signals that are consistent with demographic processes. For example, strong signals of predation were observed in regions of the trajectory where predator populations collapsed at low prey densities. Furthermore, the method provides new insight into the functioning of such systems. While signals of competition were not as strong as signals of predation, they were associated with regions in the phase portrait trajectory where the superior competitor increased rapidly while the inferior competitor remained rare.

Some of the signals identified in this study (e.g. predation signals P1, P3 and P4) have also been identified as important signals in simulated data (Sandvik *et al.* 2002) and in time-series data from freshwater populations of zooplankton (Sandvik *et al.* 2003), suggesting the presence of universal signals for some interactions. In the freshwater time series data, signals of predation could have resulted from a decrease in the prey population due to increased predation. However, lower temperatures could also have contributed to decreased prey, resulting in the same signal. These abiotic and biotic forces could not be distinguished in such complex field systems.

Constant normally distributed error			Proportional uniform error	
Average level of error added to a given time point (%)	SD	$D\%$ PC1	Range of error added to a given time point (%)	$D\%$ PC1
0 (No error)		88	0 (No error)	88
3	5689	81	3–15	82
30	56891	70	10–50	84
50	94819	46	30–150	76
70	132747	30	100–500	80
100	189638	25		
200	379276	11		

Table 4 Robustness of the AFM to the addition of constant and proportional error in time series data

Discrimination between predation and competition ($D\%$ PC1) was determined for time series data with different levels of constant and proportional error (see Methods for details).

In general, predator–prey interactions yielded stronger signals (higher ΣS_s) than competitive interactions. Competition signals appear to be less universal and strongly affected by predation. While the strongest signals associated with competition are biologically probable, indirect effects from predation on the competitively superior phage-sensitive strain (competitor-1) appeared to mask the signals we expected from competition. For example, in the absence of predation, one would expect signal C1 to be the strongest signal of competition – this signal reflects the situation where the superior competitor increases rapidly while the inferior competitor remains constant. However, in our communities, predation on the sensitive strain allowed the inferior competitor to benefit from reduced competition for nutrients during periods of intense predation on the superior competitor. Signal C4 (Fig. 3b), which occurs when the superior competitor declines rapidly from low density while the inferior competitor increases from low density, reflects this process. Signal C4 is probably due to the bacteriophage preying upon the sensitive strain, which led to a decrease in density of the sensitive strain that would not have occurred in the absence of a predator.

We also observed situations where signals could not be identified from segments of time-series data, such as in the low-productivity communities, where scores for predation and competition clustered poorly. This result was not surprising given the lack of obvious oscillations in time series segments from these communities (see Fig. 2d). However, the lack of clear signals does not suggest the absence of interactions. Our results suggest that a minimum of approximately two full predator–prey cycles (4–7 data points with two samplings daily) is required for relevant signals to be detected in our experimental systems ($D\%$ PC1 = 50 generally allows identification of signals from PCA loading plots). For signal identification the sampling frequency must capture essential dynamics. It is also important to note that for time-series segments where signals were detectable, signals were often similar and of comparable strength in full-length and shorter segments of time series.

Our comparison of systems with high and low resource levels showed that differences in dynamics due to enrichment (Bohannan & Lenski 1997, 1999, 2000) were readily detected by the AFM. The more pronounced oscillations observed in the enriched system (configuration 2_H) yielded higher discrimination between predator–prey and competition. Signals of predation in the high-productivity systems were strong and corresponded well with what one would anticipate for predator–prey interactions (i.e. counter-clockwise rotation in a phase portrait).

We have also demonstrated that small differences in bacterial competitive fitness can have detectable implica-

tions for system dynamics and that these effects could be detected by the AFM. Competitors with the largest difference in competitive fitness (competitor-1 and -3) showed the most typical and strongest signals of competition. This result is consistent with the prediction that the strain of lower competitive fitness (competitor-3) recovers more slowly from low population density than the higher-fitness competitor (competitor-2). Because the AFM measures the degree to which organisms affect one another and because the effects of competition are more severe for inferior competitors, signals of competition are stronger when the fitness differences between competitors are larger. The observation that signals of competition between two populations for a shared resource could be distinguished between communities containing different populations demonstrates the utility of the AFM.

Predator–prey models predict that small differences in bacterial competitive fitness not only affect competitive dynamics, but also predator–prey dynamics. Laboratory experiments with simple communities have demonstrated that the presence of a population invulnerable to predator attack results in a smaller predator-sensitive population and dampened predator–prey cycles, effects that can be explained by the dynamics of the shared resource (Bohannan & Lenski 1999; Bohannan *et al.* 2002). In our comparison of two communities differing in the competitive fitness of the invulnerable population, we expect the competitor of higher fitness to reduce resource levels to a greater extent than the competitor of reduce fitness. With lower resource levels available to support the edible population (competitor-1) we expect a lower growth rate of prey and, thus, a smaller predator population. Despite these clear predictions, the effects of differences in competitive fitness on the predator–prey interaction were weaker and more ambiguous than their effects on competition. Discrimination between predator–prey interactions in the two community configurations was very low along PC1 ($D\%$ PC1 = 9) and moderate along PC2 (Table 3), suggesting that the dynamics of both the bacteriophage and its prey (competitor-1) were largely insensitive to the apparently weak competitive force posed by the invulnerable competitor (competitors-2 and -3). Furthermore the difference in cumulative signal strength for predation signals between the two configurations ($\Sigma S_s = 9.30$ vs. 8.83; Table 3) was smaller than that for competition ($\Sigma S_s = 0.29$ vs. 7.00; Table 3).

Finally, the AFM was capable of detecting the invasion we observed in several communities containing the competitor of lower fitness (3_H). The results of the AFM analyses suggest that mutants of higher competitive fitness arose in the competitor-3 population and affected population dynamics. Analysis of signal strength before and after the time of presumed invasion by a mutant of higher fitness (around $t = 80$ h) further supports this conclusion.

Cumulative signal strength of competition signals was high before the time of invasion, but competition signals were absent after invasion. This trend is similar to that observed when comparing communities with a lower fitness competitor (2_H) with a higher fitness competitor (3_H). Consistent with theoretical predictions, signals of predation were also much weaker after the time of invasion. This may appear inconsistent with the fact that such a trend in predator-prey signals was not observed when 2_H and 3_H communities were compared, however, it is possible that the difference in fitness in the resistant population before and after $t = 80$ is much greater than that between competitor-2 and competitor-3.

We have demonstrated that the AFM is robust to sampling error and environmental variability, showing gradually decreasing discrimination with increasing constant error and consistently high discrimination with the addition of proportional error. The result of relatively constant discrimination with the addition of proportional error may appear counterintuitive, but it is likely that the relative differences between time points are more or less unchanged at these levels of error. Overall, these results show that the method is robust to measurement error and environmental variability. The highest levels of error here are larger than measurement errors found in many systems. A strength of PCA is its ability to extract the underlying pattern in the data; these patterns may be difficult to distort, especially if error is proportional.

There are several ways in which the AFM could be applied to field systems. The AFM can be used as a tool to further explore systems that are well-characterized. For example, the AFM can be used to detect shifts in interactions, as in our studies of well-characterized microbial experimental systems. The AFM can also be used to explore systems that are only partially characterized. For systems in which the populations that produce time series are known and characterized, but their interactions are unknown, the AFM facilitates the development of testable hypotheses about interactions between populations. Populations that interact similarly should cluster in PCA plots, and traits that are common to these populations can be further explored to elucidate their interaction. Finally, the AFM can be used to explore time series data from uncharacterized systems. The AFM could be applied to selected pairs of populations from such a system and the degree of clustering, or lack thereof, for particular pairs would identify which populations are interacting. Further exploration of characteristics shared by populations that yield clustering may suggest the type(s) of interactions. A caveat common to all these analyses is that because the AFM detects patterns in time series data, different interactions that affect populations similarly cannot be differentiated (e.g. direct and indirect interactions like competition and apparent competition).

In summary, we have shown that the AFM can yield much information from relatively few time points. Other approaches to detecting interactions in time series data (e.g. autoregressive models) generally require many more time points to establish assumed regularities in pairs of time series. Furthermore, while conventional approaches for time series analysis use the time series to develop general and predictive models for system behaviour, our approach focuses on the time series itself and how system behaviour is reflected directly in the pairs of time series. This allows the identification of interaction signatures. Statistical approaches to analysing time series data are sometimes criticized for being biologically naïve, because they treat time series data only as 'strings of numbers' (Kristoffersen 2001). However, the strength of the AFM approach is that it does not make any *a priori* assumptions about dynamic properties of the time series; clustering will occur if there are inherent dissimilarities between interactions.

We have demonstrated that the AFM is robust in identifying signals of pairwise interactions from multi-species systems. The method is capable of distilling relevant information from time series data as well as distinguishing shifts in interactions due to invasion and enrichment. This, in combination with the modest data requirements, suggests that the AFM approach is both analytically tractable and applicable in typical situations where only limited data are available. These interaction signals can potentially be used in several ways. For example, the identification of signals in phase diagrams may allow researchers to identify interactions in a community for which they have only limited data. Finally, having identified these interactions, the AFM can allow the detection of shifts in interactions due to biological or environmental change.

ACKNOWLEDGEMENTS

We gratefully acknowledge Lauren Buckley, Gerda Saxer, Samantha Forde, Clara Davis, Claire Horner-Devine and Ben Kerr for critical and constructive comments. We also wish to thank Harald Pleym for invaluable assistance in Maple programming. This work was funded by a National Science Foundation grant (DEB-0129942) to BB.

REFERENCES

- Berryman, A.A. (2001). Functional web analysis: detecting the structure of population dynamics from multi-species time series. *Basic Appl. Ecol.*, 2, 311–321.
- Berryman, A.A. & Turchin, P. (2001). Identifying the density-dependent structure underlying ecological time series. *Oikos*, 92, 265–270.
- Bohannan, B.J.M. & Lenski, R.E. (1997). Effect of resource enrichment on a chemostat community of bacteria and bacteriophage. *Ecology*, 78, 2303–2315.